Pharmacological Research 227 (2026) 108189

Contents lists available at ScienceDirect

Pharmacological Research

journal homepage: www.elsevier.com/locate/yphrs

SGK1-inhibition restores cardiac repolarization in LQT2 rabbits and LQT3 mice by reducing late sodium current

Miriam Barbieri [a,1], Simona Casini [b,c,1], Julien Louradour [a], Tanja M. de Waal [b,c], Nicolò Alerni [a], Arie O. Verkerk [b,c,d], Federica Giannetti [e], Luca Sala [e,f], Philip T. Sager [g,h], Saumya Das [g,i], Gideon Koren [j], Manfred Zehender [k], Michael Brunner [k,l], Lior Gepstein [m], Lia Crotti [e,n], Peter J. Schwartz [e], Arthur A.M. Wilde [c,o,p], Katja E. Odening [a,k,*,2], Carol A. Remme [b,c,**,2]

[a] Translational Cardiology, Department of Physiology, University of Bern, and Department of Cardiology, University Hospital Bern Bühlplatz 5, 3012 Bern, Switzerland.
[b] Department of Experimental Cardiology, Heart Centre, Amsterdam UMC location University of Amsterdam, Meibergdreef 9, Amsterdam 1105 AZ, the Netherlands
[c] Amsterdam Cardiovascular Sciences, Cardiomyopathy & Arrhythmia, Amsterdam, the Netherlands
[d] Department of Medical Biology, Amsterdam UMC location University of Amsterdam, Meibergdreef 9, Amsterdam 1105 AZ, the Netherlands
[e] Istituto Auxologico Italiano IRCCS, Center for Cardiac Arrhythmias of Genetic Origin and Laboratory of Cardiovascular Genetics, Milan, Italy
[f] Department of Biotechnology and Biosciences, University of Milano-Bicocca, Milan, Italy
[g] Thryv Therapeutics Inc., Montreal, Canada
[h] Cardiovascular Research Institute, Stanford University, Palo Alto, CA, USA
[i] Massachusetts General Hospital, Harvard Medical School, Boston, MA, USA
[j] Cardiovascular Research Center, Brown University, Providence, RI, USA
[k] Department of Cardiology and Angiology I, University Heart Center Freiburg, University Medical Center Freiburg, Freiburg, Germany
[l] Department of Cardiology and Intensive Care, St. Josefskrankenhaus Freiburg, Freiburg, Germany
[m] Cardiology Department, Rambam Health Care Campus and Rappaport Faculty of Medicine, Technion – Israel Institute of Technology, Haifa, Israel
[n] Department of Medicine and Surgery, University of Milano-Bicocca, Milan, Italy
[o] Department of Clinical Cardiology, Heart Centre, Amsterdam UMC location University of Amsterdam, Meibergdreef 9, Amsterdam 1105 AZ, the Netherlands
[p] European Reference Network for rare, Low prevalence and complex diseases of the heart: ERN GUARD-Heart' (ERN GUARDHEART), the Netherlands

ARTICLE INFO

Keywords:
Long QT syndrome
SGK1-inhibition
Late sodium current
Cardiac repolarization
Antiarrhythmic mechanisms
Transgenic animal models

ABSTRACT

Current management does not fully prevent arrhythmias in long QT syndrome (LQTS), underscoring a need for novel therapies. Here, we investigated potential beneficial effects of serum/glucocorticoid-regulated-kinase-1 (SGK1)-inhibition in different LQTS animal models. Ventricular cardiomyocytes (CMs) isolated from wild-type (WT), LQT1 (*KCNQ1*-Y315S) and LQT2 (*KCNH2*-GS628S) rabbits, and WT and LQT3 (*Scn5a*-1798insD$^{+/-}$) mice were incubated for 2–4 h with SGK1-inhibitor (SGK1-inh, 300 nM or 3 μM) or vehicle to assess its effects on action potential duration (APD) and late sodium current (late I_{Na}). Whole heart experiments were performed to investigate SGK1-inh effects on QT duration (rabbits) and ventricular effective refractory periods (ERP, mice). Late I_{Na} was enhanced in LQT2 and LQT3 CMs, but not in LQT1. SGK1-inh reduced late I_{Na} in LQT2 (by 60%) and LQT3 (by 33%) CMs, but not in LQT1. Consequently, SGK1-inh shortened APD in LQT2 (by 25%) and LQT3 CMs (by 23%) restoring these to WT levels, but did not affect APD in LQT1. The proarrhythmic marker short-term-variability of APD was increased in LQT2 and LQT3, and was reduced by SGK1-inh in LQT2 (by 48%) and LQT3 (by 49%) CMs. Additionally, SGK1-inh decreased triggered APs in LQT3 CMs. Finally, SGK1-inh perfusion in *ex vivo* hearts shortened QT-interval in LQT2 and decreased ventricular ERP in LQT3, restoring them to WT levels. In conclusion, late I_{Na} is increased in LQT2 rabbits and LQT3 mice, but not in LQT1 rabbits. SGK1-

* Corresponding author at: Translational Cardiology, Department of Physiology, University of Bern, and Department of Cardiology, University Hospital Bern Bühlplatz 5, 3012 Bern, Switzerland.
** Correspondence to: Department of Clinical and Experimental Cardiology/Heart Centre, Academic Medical Centre, University of Amsterdam, Meibergdreef 9, Amsterdam 1105 AZ, the Netherlands.
E-mail addresses: katja.odening@unibe.ch, katja.odening@insel.ch (K.E. Odening), c.a.remme@amsterdamumc.nl (C.A. Remme).
[1] Shared first authors
[2] shared last & corresponding authors

https://doi.org/10.1016/j.phrs.2026.108189
Received 16 February 2026; Received in revised form 31 March 2026; Accepted 10 April 2026
Available online 15 April 2026

inhibition shortens APD/QT and reduces proarrhythmic risk in LQT2 and LQT3 CMs by suppressing enhanced late I_{Na}, indicating potential therapeutic benefit.

1. Introduction

Congenital long QT syndrome (LQTS) is an inherited cardiac disorder, associated with life-threatening Torsade-de-Pointes ventricular arrhythmias that can lead to syncope and sudden cardiac death (SCD), often occurring in apparently healthy and relatively young individuals [1–3]. LQTS has a heterogenous genetic basis, with LQT1, LQT2 and LQT3 being the most prevalent subtypes [4,5]. LQT1 and LQT2 result from loss-of-function (LOF) variants in *KCNQ1* or *KCNH2* genes, encoding the α-subunits carrying the slow and rapid delayed rectifier potassium currents (I_{Ks} and I_{Kr}), respectively [6]. LQT3 results from gain-of function (GOF) variants in the *SCN5A* gene, encoding the α-subunit of the cardiac sodium channel $Na_v1.5$, causing an impaired channel inactivation leading to an enhanced late sodium current (I_{Na}) [7]. The net result of all these pathogenic variants is prolongation of the ventricular action potential duration (APD) and QT interval [1].

Current treatment strategies aim to reduce arrhythmogenic triggers through beta-blockade or left cardiac sympathetic denervation, sodium channel blockers like mexiletine, and lifestyle modifications, e.g., avoidance of QT-prolonging drugs (www.crediblemeds.org) [1,8,9]. In high-risk patients, implantable cardioverter-defibrillators (ICDs) are used to terminate life-threatening arrhythmias once they occur [10]. However, the frequent adverse side effects caused by ICDs [11] and the incomplete protection against arrhythmic events especially in selected high-risk groups [12] and more often in LQT2 and LQT3 than in LQT1, highlight the unmet need for novel, more effective, mechanism-based therapeutic strategies. Targeting downstream proarrhythmic effects caused secondarily by the prolonged cardiac repolarization, particularly those affecting intracellular Na^+ and Ca^{2+} homeostasis, offers an interesting opportunity. One such approach involves the pharmacological inhibition of the serum-and-glucocorticoid-regulated kinase 1 (SGK1), whose over-activation has previously been linked to enhanced late I_{Na} and prolonged APD [13]. SGK1-inhibition has previously been shown to shorten APD in human-induced pluripotent stem cell-derived cardiomyocytes (hiPSC-CMs) from LQT1, LQT2, and LQT3 patients [14–16]. In addition, we recently characterized the effects of a novel SGK1-inhibitor (SGK1-inh) using a comprehensive set of *in vitro* (hiPSC-CMs), advanced human cardiac cell sheets (hiPSC-CCS), and cardiomyocytes (CMs) isolated from transgenic rabbit models of LQT1 and LQT2 [17], and demonstrated that SGK1-inh shortened APD in all LQT2 models tested (independently of the disease-causing variant), but produced variable effects on APD in three different LQT1 variants, suggesting a gene- and variant-specific efficacy of SGK1-inhibition in LQTS. In the present study, we directly investigated the effect of SGK1-inh on one of its proposed downstream targets, late I_{Na}, using our transgenic LQT1 and LQT2 rabbit models [18] and LQT3 mouse model [19], and explored for the first time its potential antiarrhythmic effects.

2. Methods

2.1. Ethical use of animal models

Adult transgenic LQT1 (*KCNQ1*-Y315S, loss of I_{Ks}) LQT2 (*KCNH2*-G628S, loss I_{Kr}) [18] and wild-type (WT) New Zealand White rabbits of both sexes, aged 3 months to 1 year, were used in this study. All experiments were performed in compliance with EU legislation (directive 2010/63/EU), and animal housing and handling were in accordance with FELASA standards and the Swiss Animal Welfare Ordinance, after approval by the Cantonal Veterinary Office and the Animal Welfare Officer (Kanton Bern, animal licenses BE132–20, BE74–23). Heterozygous *Scn5a*-1798insD mice (129P2 background) were generated as previously described [19,20]. All experiments were performed in adult (5–7 months old) *Scn5a*-1798insD male mice and their WT littermates as control in accordance with governmental and institutional guidelines for animal use in research (Animal Care and Use Committees of the University of Amsterdam, license AVD11400202115027). All animal experiments comply with the ARRIVE guidelines.

2.2. Compounds

The SGK1-inh (provided by Thryv Therapeutics) was dissolved in DMSO (vehicle) to obtain a 10 mM stock solution and further diluted in external solutions to obtain the following concentrations: 300 nM (for LQT3 mice experiments) and 3 μM (for LQT1 and LQT2 rabbit experiments). These concentrations were optimized independently for the different LQTS subtypes to achieve comparable effects [17]. As stated in our previous work [17], its selectivity for SGK1-inhibition had been examined in a biochemical assay, which assessed the kinase reactivity in a 50-kinase panel, and in a cell-based *in vitro* screening assay. The results indicated that SGK1-inh is highly selective. In all solutions used, the final DMSO vehicle concentration was $< 0.001\%$, found to be devoid of effect in isolated CMs and *ex vivo* whole hearts. For all measurements, SGK1-inh was compared to DMSO-containing solution (vehicle).

2.3. Rabbit heart extraction

Transgenic LQT1, LQT2 and WT rabbits (males and females) were anaesthetized with an intramuscular (IM) injection of ketamine S (Ketanest S®, Pfizer, 12.5 $mg{\cdot}kg^{-1}$ body weight) and xylazine (Rompun®, Bayer, 3.75 $mg{\cdot}kg^{-1}$ body weight), as this anaesthesia does not affect cardiac repolarization [21]. After deep anaesthesia (no eye or pinch reflexes), heparin (liquemin®, 500 IU) was injected intravenously (IV) in the ear vein to prevent clotting upon heart extraction. Terminal euthanasia was conducted by IV injection of pentobarbital (Esconarkon®, 150 $mg{\cdot}kg^{-1}$ body weight), and hearts were rapidly excised and immersed in a cold (4°C) Tyrode solutions (in mM: 135 NaCl, 0.4 NaH_2PO_4, 5 KCl, 10 HEPES, 1 $MgCl_2$, 1.8 $CaCl_2$, 10 glucose, 10 creatine, and 20 taurine, adjusted to pH=7.4 with NaOH) before ventricular CMs isolation or *ex vivo* whole heart experiments.

2.4. Rabbit cardiomyocytes isolation

After extraction, hearts were rapidly cannulated and retrogradely perfused by the aorta and mounted on a Langendorff perfusion system. Hearts were perfused with an oxygenated, body temperature (37°C) Tyrode solution supplemented with 0.1 mM EGTA for 5–7 min to stop the contraction, followed by a 20–25 min collagenase digestion (Worthington type I, 200 mg) in 80 μM Ca^{2+} Tyrode solution [22]. Thereafter, the left ventricles were dissected and cut into small pieces that were further digested in sequential 3 min steps with collagenase (Worthington type I, 50 mg) in 80 μM Ca^{2+} Tyrode solution supplemented with 15 mM bovine serum albumin (BSA). Isolated ventricular CMs were maintained in a 0.2 mM Ca^{2+} Tyrode solution and subsequently incubated at room temperature with 3 μM SGK1-inh or DMSO (vehicle). CMs were used for patch-clamp analysis 2–4 h after the start of incubation.

2.5. Mouse heart extraction

After receiving an intraperitoneal injection of 20 μL heparin (5000 IU/mL), mice were sacrificed by cervical dislocation under anaesthesia (4% isoflurane in O_2), and the heart was excised and immersed in a modified Tyrode solution (in mM: 140 NaCl, 5.4 KCl, 1.8 $CaCl_2$, 1.0

$MgCl_2$, 5.5 glucose, and 5.0 HEPES, adjusted to pH 7.4 with NaOH), and used either for ventricular CMs isolation or *ex vivo* whole heart experiments.

2.6. Mouse cardiomyocyte isolation

Isolated hearts were cannulated and retrogradely perfused for 10 min in a Langendorff system with oxygenated modified Tyrode solution (37°C) described above. Next, the heart was perfused for 10 min with Ca^{2+}-free modified Tyrode solution containing 0.01 mM $CaCl_2$, supplemented with 10.7 mM creatine monohydrate (Sigma, C3630). Subsequently, the heart was digested using Liberase TM (0.18–0.21 U/mL; Roche) and elastase from porcine pancreas (2.5–2.9 U/mL; SERVA) in Ca^{2+}-free modified Tyrode solution for around 12 min. The heart was then placed in Ca^{2+}-free modified Tyrode solution containing 1% BSA (Sigma-Aldrich). Atria and right ventricular free wall were removed, and the left ventricle was mechanically dissociated to obtain single CMs. Isolated CMs were carefully washed with Ca^{2+}-free modified Tyrode solution to remove BSA, and subsequently incubated at room temperature with 300 nM SGK1-inh or DMSO (vehicle). Single CMs were used for patch-clamp analysis 2–4 h after the start of incubation.

2.7. Patch-clamp analysis

2.7.1. Data acquisition and analysis

Voltage and current clamp recordings were performed at physiological temperature (37 °C) in isolated mouse and rabbit left ventricular CMs. Late I_{Na} and action potentials (APs) were measured with the ruptured and perforated patch-clamp technique, respectively, using an Axopatch 200B amplifier (Molecular Devices, USA). Voltage control, data acquisition and analysis were performed with pClamp/Clampfit (Molecular Devices, version 10.6 for the mouse experiments and 11.1 for the rabbit experiments). Borosilicate glass patch pipettes with a tip resistance of 2–2.2 MΩ were used. Series resistance and cell membrane capacitance were compensated for $\geq$ 80%. APs were filtered at 5 kHz and digitized at 40 kHz in mouse CMs and at 20 kHz in rabbit CMs. Late I_{Na} was filtered at 2 kHz and digitized at 1 kHz in mouse and rabbit CMs.

2.7.2. Late I_{Na} measurements

For late I_{Na} recordings, pipettes were filled with a solution containing (in mM): 3.0 NaCl, 133 CsCl, 2.0 $MgCl_2$, 2 Na_2-ATP, 2 TEACl, 10 EGTA, and 5 HEPES (adjusted to pH=7.2 with CsOH). Ventricular CMs were constantly perfused with bath solution containing (in mM): 130 NaCl, 10 CsCl, 1.8 $CaCl_2$, 1.2 $MgCl_2$, 11 glucose and 5.0 HEPES (pH 7.4 with CsOH). The bath solution contained 5 μM nifedipine to block the L-type calcium current). In rabbit CMs, late I_{Na} was measured using a squared 300 ms depolarizing step from a holding potential of −100 mV to −20 mV, with a cycle length of 5 s. The same protocol was subsequently applied in the presence of the specific late I_{Na}-blocker ranolazine (100 μM). Late I_{Na} was then defined as ranolazine-sensitive current by subtracting the two traces. Late I_{Na} was measured between 250 and 300 ms after the initiation of the depolarizing pulse (see insets in Fig. 1A). In mouse CMs late I_{Na} was measured as 30 μM tetrodotoxin (TTX)-sensitive current, using a descending ramp protocol from a holding potential of −90 mV (cycle length of 5 s; see insets in Fig. 1C). Current densities were calculated dividing the current amplitude by the cell membrane capacitance. Potentials were not corrected for the estimated change in liquid junction potential (6 mV) [23].

2.7.3. Action potential measurements

Mouse and rabbit APs were measured using the modified Tyrode solution described above. Pipettes were filled with (in mM): 125 K-gluconate, 20 KCl, 5 NaCl, 0.44 amphotericin-B, 10 HEPES, adjusted to pH 7.2 with KOH). APs were elicited at 1 Hz (rabbit CMs) or 2 Hz (mouse CMs) by 3 ms, ~1.2 × threshold current pulses through the patch pipette. Resting membrane potential (RMP), AP amplitude (APA), maximal AP upstroke velocity (V_{max}), and AP duration (APD) at 20, 50, and 90% repolarization (APD_{20}, APD_{50}, and APD_{90}, respectively) were analysed. Data from 10 consecutive APs were averaged and potentials were corrected for the calculated liquid junction potential (15 mV) [23]. In mouse CMs, triggered activity, i.e., delayed afterdepolarizations (DADs) and triggered action potentials (TAPs), was assessed using a fast pacing protocol [24] consisting of 20 elicited APs at a frequency of 5 Hz followed by a 10 s pause. Three consecutive traces were used to analyse the average amount of DADs and TAPs during the pause.

2.8. Short-term variability of APD_{90} analysis

Series of 10 consecutive APs in rabbit and mouse CMs were analysed to estimate short-term variability of APD_{90} (STV) according to the following formula: $STV = \Sigma(|APD_{n+1} - APD_n|)/[(n_{beats} - 1) \times \sqrt{2}]$ where APD_n and APD_{n+1} indicate the durations of the n^{th} and $(n+1)^{th}$ APs, and n_{beats} denotes the total number of consecutive beats analysed [25].

2.9. Rabbit ex vivo whole heart experiments

After extraction, hearts were rapidly mounted on a Langendorff perfusion system (IH5, Hugo Sachs Electronic-Harvard Apparatus, Hugstetten, Germany) via cannulation of the aorta and perfused with oxygenated, body temperature (37°C) Krebs-Henseleit (KH) solution consisting of (in mM): 118 NaCl, 4.7 KCl, 1.2 KH_2PO_4, 24.9 $NaHCO_3$, 1.8 $CaCl_2$, 0.8 $MgSO_4$, 5.6 glucose, and 2 Na-pyruvate, adjusted to pH 7.4 using HCl. Perfusion of the heart was kept at a constant flow of 50 mL/min and a constant aortic pressure of 80 mmHg. Electrocardiograms were recorded via three electrodes positioned to the left side, right side and apex of the heart to measure the three bipolar leads I, II, III, and the unipolar leads aVR, aVL, and aVF [26,27]. A latex balloon was inserted in the left ventricle and coupled to a pressure transducer (Hugo Sachs Electronic-Harvard Apparatus, Hugstetten, Germany) to measure the left ventricle pressure (LVP), used as internal control for checking heart viability, with a fixed end diastolic pressure of 8 mmHg. Complete electrical dissociation of atria and ventricles was performed by electrocauterizing the atrioventricular (AV) node with an electrocauter to enable a slow (< 2.5 Hz) ventricular escape rhythm [28]. QT interval was measured during LV pacing (2.5 Hz) in control condition (baseline, DMSO perfusion) and after 60 min perfusion of 3 μM SGK1-inh. 15 subsequent QT intervals were measured in the last minute of DMSO and SGK1-inh perfusion and averaged. Temporal control experiments solely with DMSO application were performed to check potential temporal changes in QT interval.

2.10. Mouse ex vivo whole heart experiments

The heart was excised, cannulated and mounted on a Langendorff perfusion set-up, and perfused at 37°C with a solution containing (in mM): 128 NaCl, 4.7 KCl, 1.45 $CaCl_2$, 0.6 $MgCl_2$, 26 $NaHCO_3$, 0.4 NaH_2PO4, and 11 glucose (pH maintained at 7.4 by equilibration with a mixture of 95% O_2 and 5% CO_2). Electrocardiograms were recorded via three electrodes positioned to the left side, right side and apex of the heart to measure the three bipolar leads I, II, III. The effective refractory period (ERP) was measured during right ventricular pacing in control conditions (baseline, DMSO) and after 60 min perfusion of 300 nM SGK1-inh. ERP was determined by reducing the coupling interval of a premature stimulus (after 36 stimuli at basic cycle length of 150 ms) in steps of 5 ms until activation of the ventricle failed. Average of two subsequent ERP were calculated. Temporal control experiments solely with DMSO application were also performed to check potential temporal changes in ERP.

2.11. Statistics

Statistical analysis was performed using Prism 10.6.1 (GraphPad

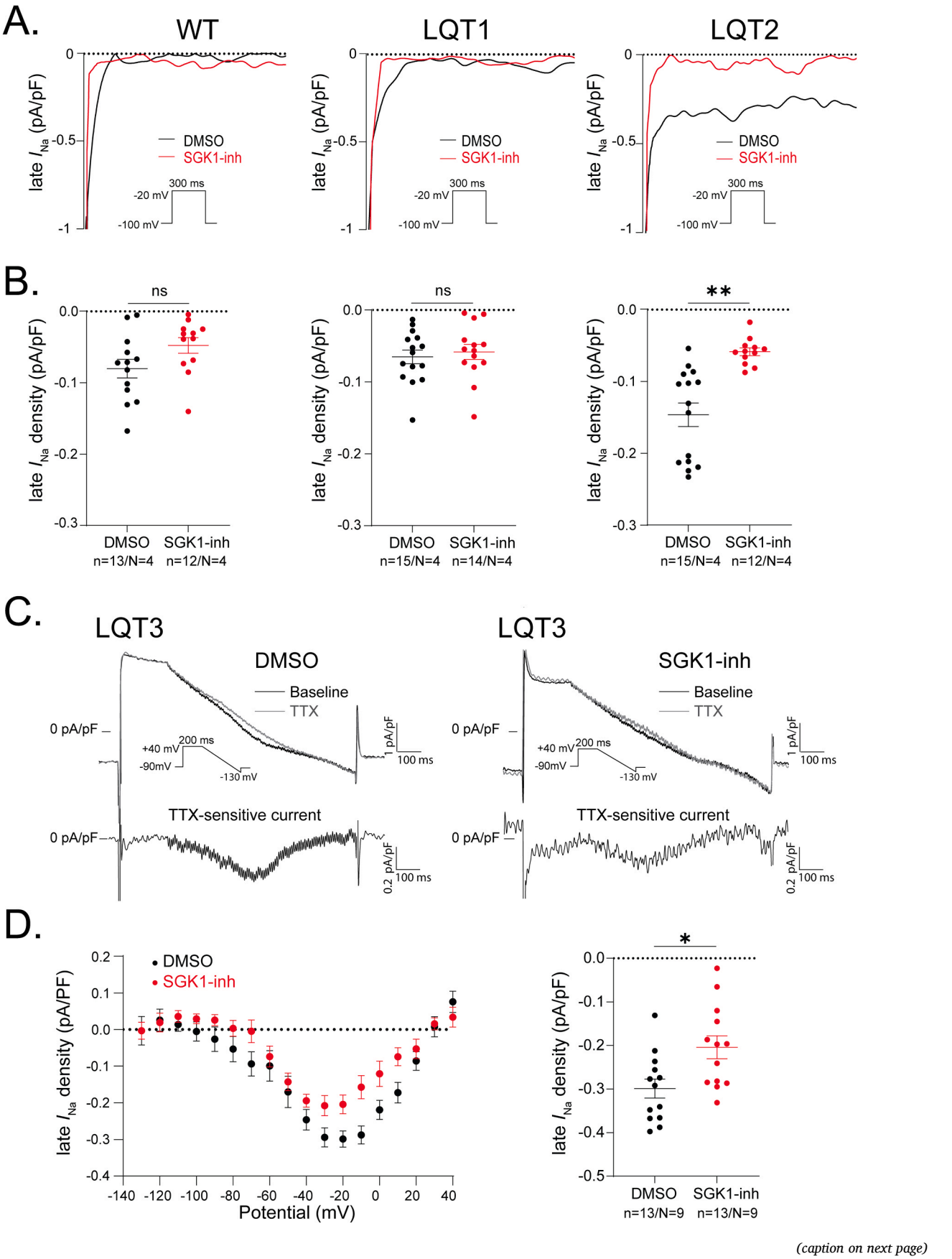

(caption on next page)

Fig. 1. Effects of SGK1-inh on late I_{Na} in isolated cardiomyocytes (CMs) from rabbits and mice. (A) Representative example of ranolazine-sensitive late I_{Na} traces recorded in WT, LQT1 and LQT2 in isolated rabbit CMs after 2–4 h of incubation with DMSO (black line, vehicle), or SGK1-inh (red line, 3 μM). Ranolazine-sensitive current was obtained by subtraction of the current before and after ranolazine (100 μM) bath application and was measured between 250 and 300 ms after the initiation of the squared pulse (see insets). (**B**) Average late I_{Na} density in WT, LQT1 and LQT2 CMs after 2–4 h of incubation with DMSO or SGK1-inh. (**C**) Representative late I_{Na} recordings obtained using a descending ramp protocol (see insets) in mouse LQT3 CMs before (baseline, black) and after application of TTX (30 μM, grey), after 2–4 h of incubation with DMSO or SGK1-inh (300 nM). TTX-sensitive current was obtained by subtraction of the current before and after TTX bath application. (**D**) Average current-voltage (I-V) relationships for TTX-sensitive currents (left panel) and late I_{Na} density measured at −20 mV (right panel) in LQT3 CMs after incubation with DMSO or SGK1-inh. n, number of CMs, N, number of animals. ***p < 0.01, *p < 0.05, nested t-test; ns = non-significant.*

Software, USA). Data are expressed as mean ± standard error of the mean (S.E.M.). Electrophysiological measurements (late I_{Na}, APD_{90}, STV of APD_{90}, TAPs and DADs) were analysed using a hierarchical statistical approach to account for the non-independence of multiple cardiomyocytes isolated from the same animal. Cells were treated as nested within individual animals, with the animal considered the independent unit. Nested *t*-test or nested one-way ANOVA were applied where appropriate, as detailed in the figure legends. For *ex vivo* parameters (QT interval and ERP), normality was assessed using the Shapiro-Wilk test, and parametric or non-parametric testes were applied accordingly. $P < 0.05$ was considered statistically significant.

3. Results

3.1. SGK1-inh reduces enhanced late sodium current in LQT2 rabbit and LQT3 mouse cardiomyocytes

Enhanced late I_{Na} is a well-established feature of LQT3 and was previously demonstrated in our *Scn5a*-1798insD mouse model [19]. We here explored whether late I_{Na} is also enhanced in the context of LQT1 and LQT2, employing our transgenic rabbit models. Late I_{Na} was found to be unchanged in LQT1 rabbit CMs as compared to WT (LQT1: −0.07 ± 0.01 pA/pF versus WT: −0.08 ± 0.02 pA/pF; *ns*; Suppl. Figure S1A,C) while it was significantly increased in LQT2 rabbit CMs (LQT2: −0.15 ± 0.02 pA/pF versus WT: −0.08 ± 0.02 pA/pF; $p < 0.05$; Suppl. Figure S1B,D). We next investigated whether SGK1-inh can reduce late I_{Na} in LQT1, LQT2 and LQT3 CMs. SGK1-inh (3 μM, 2–4 h) significantly reduced late I_{Na} in LQT2 CMs, inducing an average 60% decrease at −20 mV (DMSO: −0.15 ± 0.02 pA/pF versus SGK1-inh: −0.06 ± 0.01 pA/pF; $p < 0.01$); in contrast, SGK1-inh did not affect late I_{Na} in WT or LQT1 CMs, both of which remained at baseline levels (Fig. 1A,B). Similarly, incubation of LQT3 mouse CMs with SGK1-inh (300 nM, 2–4 h) significantly reduced late I_{Na} by 33% at −20 mV (DMSO: −0.3 ± 0.02 pA/pF versus SGK1-inh: −0.2 ± 0.02 pA/pF; $p < 0.05$; Fig. 1C, D). Taken together, these data indicate that SGK1-inh targets late I_{Na} and reduces its magnitude in the context of both LQT2 and LQT3.

3.2. SGK1-inh shortens action potential duration in LQT2 rabbit and LQT3 mouse cardiomyocytes

To investigate whether the SGK1-inh mediated decrease in late I_{Na} could reduce or even normalize repolarization in LQTS, we tested its effect on APD in isolated CMs from WT, LQT1 and LQT2 rabbits and from WT and LQT3 mice. APD_{90} and APD_{50} were significantly prolonged in LQT1 and LQT2 CMs as compared to WT CMs (APD_{90}: $p < 0.001$; APD_{50}: LQT1: $p < 0.05$; LQT2: $p < 0.01$; Suppl. Table S1), similarly as previously described [28], while no differences were observed in APA, V_{max} and RMP (Suppl. Table S1). Finally, in line with our previous findings [19], LQT3 CMs exhibited a significantly increased APD_{90} relative to WT($p < 0.01$, Suppl. Table S2).

SGK1-inh (300 nM for mouse CMs, 3 μM for rabbit CMs) significantly reduced APD_{90} and APD_{50} in LQT2 CMs by 25% ($p < 0.001$ and $p < 0.05$, respectively; Fig. 2A,B; Suppl. Table S1) and APD_{90} in LQT3 CMs by 23% ($p < 0.05$; Fig. 2C,D), normalizing them towards the WT level (Suppl. Figure S2A,C). In contrast, in CMs from WT and LQT1 rabbits and from WT mice, no effect of SGK1-inh on APD_{90} was observed (Fig. 2). Similarly, SGK1-Inh had no effect on APA, V_{max} and RMP across all rabbit and mouse genotypes (Suppl. Tables S1 and S2). In conclusion, SGK1-inh is able to shorten APD in LQT2 and LQT3 CMs and restore it towards WT level but has no effect in WT CMs or LQT1 rabbit CMs, consistent with the absence of increased late I_{Na} in this model.

3.3. SGK1-inh has antiarrhythmic effects in LQT2 and LQT3 cardiomyocytes

To explore if SGK1-inh has an antiarrhythmic effect at the cellular level, we tested its effect on the short-term variability (STV) of APD_{90} - a marker of enhanced arrhythmic risk [29] - in isolated CMs from WT, LQT1 and LQT2 rabbits and from WT and LQT3 mice. At baseline, LQT2 CMs exhibited a higher STV than WT CMs ($p < 0.01$; Suppl. Table S1), whereas LQT1 CMs did not (Suppl. Table S1). Similarly to LQT2 CMs, LQT3 mouse CMs presented a higher STV compared to WT CMs ($p < 0.05$; Suppl. Table S2).

SGK1-inh significantly reduced STV in LQT2 ($p < 0.05$; Fig. 3A,C; Suppl. Table S1) and in LQT3 CMs ($p < 0.01$; Fig. 3B,D; Suppl. Table S2), normalizing them towards the WT level (Suppl. Figure S2B,D; Suppl. Tables S1 and S2). In contrast, no effect was observed in CMs from WT mice (Fig. 3B,D; Suppl. Table S2), WT rabbits or LQT1 rabbits (Fig. 3A,C; Suppl. Table S1).

In addition, direct assessments of potential antiarrhythmic effects on triggered activity were conducted in CMs from LQT3 mice. The fast pacing protocol used to quantify DADs and TAPs consisted in applying 20 pulses at a frequency of 5 Hz followed by a 10 s pause in LQT3 CMs incubated with DMSO (Fig. 4A top panel) or SGK1-inh (300 nM, Fig. 4A, bottom panel). While SGK1-inh treatment did not affect DADs occurrence (count), it significantly reduced the number of triggered APs as compared to the DMSO group ($p < 0.05$; Fig. 4B), further underscoring its antiarrhythmic potential.

3.4. SGK1-inh improves ventricular repolarization in isolated LQT2 and LQT3 hearts

Given the observed effects of SGK1-inh on APD in LQT2 rabbit CMs, we further tested whether SGK1-inh could shorten/normalize the QT interval *ex vivo* during fixed pacing in Langendorff-perfused hearts. WT and LQT2 hearts were first perfused with DMSO to establish baseline QT intervals from ECG recordings, followed by 60 min perfusion with SGK1-inh.

Similarly to the observations in isolated CMs, SGK1-inh significantly shortened the QT interval in LQT2 ($p < 0.001$; Fig. 5B), normalizing it towards the WT level (Suppl. Figure S3A). In contrast, no effect on WT rabbit hearts was observed (Fig. 5A).

As QT intervals are harder to assess in mice than in rabbits due to the differences in T wave morphology, we measured the ventricular ERP in *ex vivo* isolated mouse hearts as a marker of repolarization. The ERP was determined by reducing the coupling interval of a premature stimulus (after 36 stimuli at basic cycle length of 150 ms) in steps of 5 ms until activation of the ventricle failed. Ventricular ERP was significantly longer in LQT3 hearts as compared to WT ($p < 0.05$; Suppl. Figure S3B), as previously described [19]. Perfusion of the explanted hearts with SGK1-inh (60 min, 300 nM) did not affect ERP in WT (Fig. 5C), while it significantly shortened the ERP in LQT3 hearts and restored it to WT levels ($p < 0.05$; Fig. 5D; Suppl. Figure S3B).

To exclude that the observed shortening of QT interval or ERP

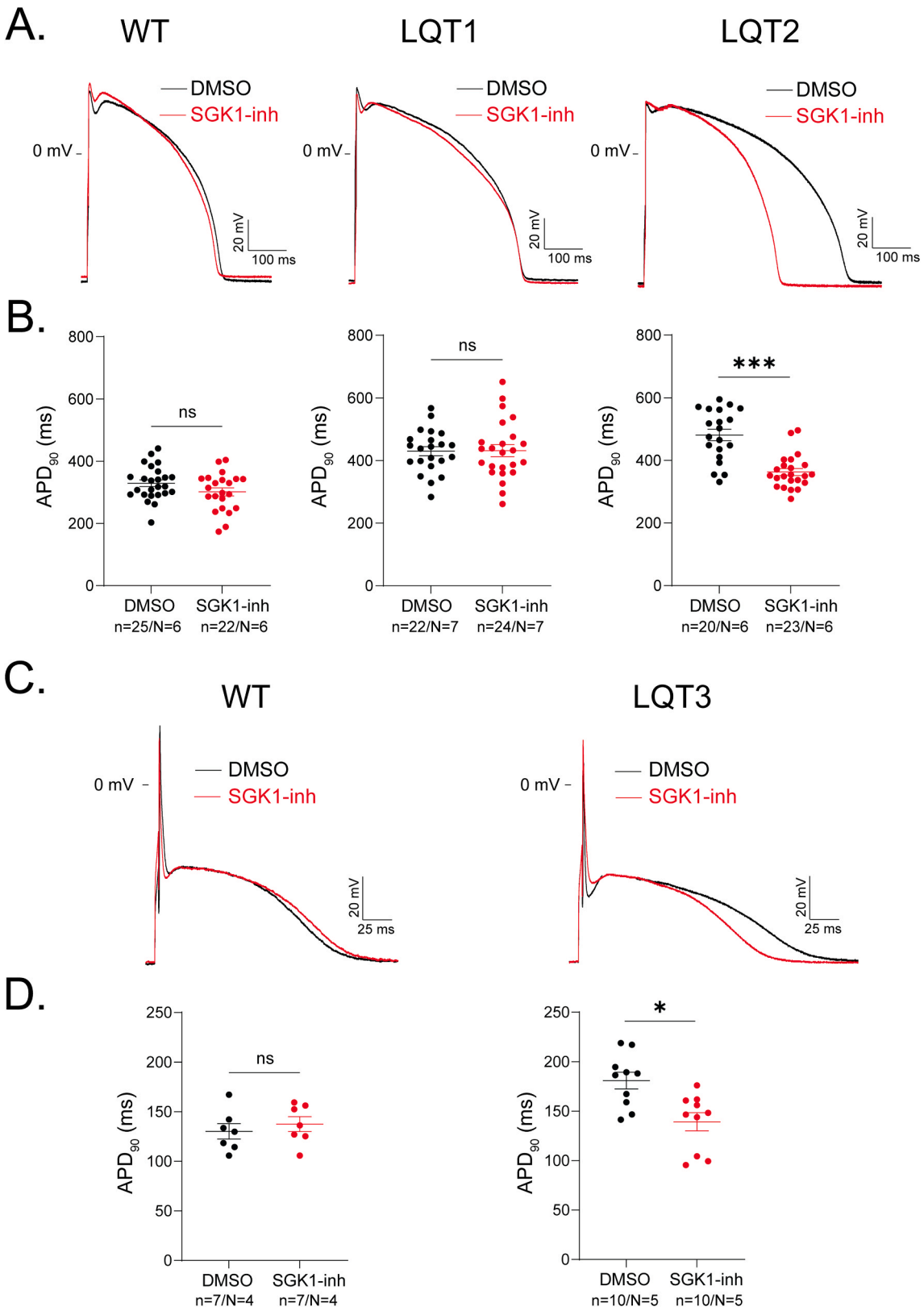

Fig. 2. Effects of SGK1-inh on APD_{90} in isolated rabbit and mouse CMs. (A) Representative AP traces recorded at the stimulation frequency of 1 Hz in WT, LQT1 and LQT2 isolated rabbit CMs after 2–4 h of incubation with DMSO (vehicle) or SGK1-inh (3 μM). (**B**) Average values for APD at 90% repolarization (APD_{90}) after incubation with DMSO (vehicle) or SGK1-inhibitor (3 μM) in WT, in LQT1 and LQT2 rabbit CMs. (**C**) Representative AP traces recorded at the stimulation frequency of 2 Hz in WT and LQT3 isolated mouse CMs after 2–4 h of incubation with DMSO (vehicle) or SGK1-inh (300 nM). (**D**) Average values for APD_{90} in WT and LQT3 mouse CMs incubated with DMSO or SGK1-inh (300 nM). n, number of CMs, N, number of animals. ****p < 0.001, *p < 0.05, nested t-test; ns = non-significant.*

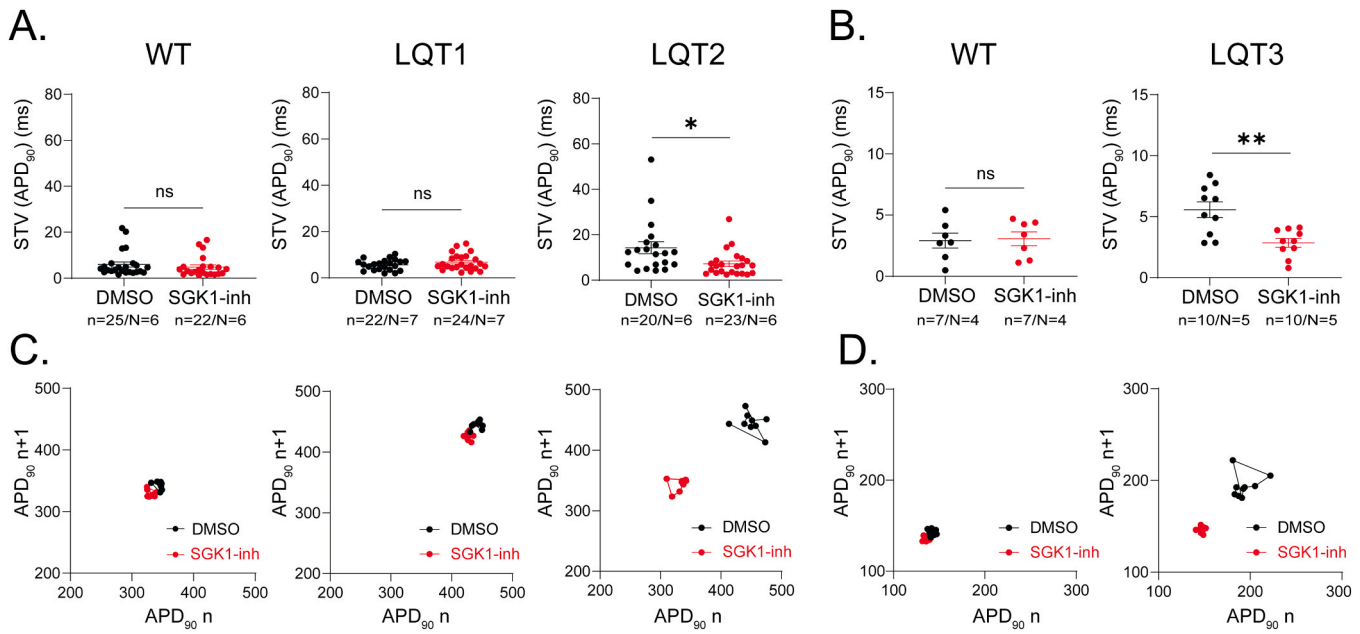

Fig. 3. SGK1-inh exerts an antiarrhythmic effect at the cellular level in LQT2 and LQT3 CMs. (A,C) Average values of short-term variability (STV) of the APD_{90} (**A**) and examples of short-term variability of the APD_{90} in one cell visualized with a Poincaré plot (**C**) in WT, LQT1, and LQT2 rabbit cardiomyocytes after 2–4 h of incubation with DMSO or SGK1-inh (3 μM). (**B**,**D**) Average values for STV of APD_{90} (**B**) and examples of short-term variability of the APD_{90} in one cell visualized with a Poincaré plot (**D**) in WT and LQT3 mouse cardiomyocytes after 2–4 h of incubation with DMSO or SGK1-inh (300 nM). Average values were calculated using 10 consecutive APs. n, number of CMs, N, number of animals. *$p < 0.5$, **$p < 0.01$, nested t-test; ns = non-significant.*

secondary to acute SGK1-inh treatment was due to a time-dependent effect, we performed the same experiments with a temporal control (DMSO perfusion only, for a similar duration). No significant temporal change was observed in QT interval or ERP (Suppl. Figure S4). These observations indicate that the QT or ERP shortening during SGK1-inh perfusion is due to the late I_{Na}-blocking effect of the compound itself and not attributable to any time-induced QT/ERP shortening.

Taken together, these results indicate that SGK1-inh is able to shorten the QT interval in LQT2 and ERP in LQT3 hearts, respectively, therefore confirming that the shortening of repolarization observed at the cellular level is preserved at the whole heart level.

4. Discussion

In the present study, we expanded our prior work on the effects of SGK1-inhibition on cardiac repolarization in LQTS by investigating its impact on one of the proposed downstream targets, i.e. late I_{Na}. For this purpose, we utilized our LQT1 and LQT2 rabbit [18] and LQT3 mouse [19] models, which accurately mimic the disease phenotype on all levels thus allowing us to investigate SGK1-inh's efficacy on cellular and whole heart levels. We showed that i) in addition to LQT3, late I_{Na} is also increased in LQT2, but not in LQT1 rabbit CMs, ii) SGK1-inh attenuated late I_{Na}, decreased APD and displayed antiarrhythmic effects in LQT2 and LQT3 CMs but not in LQT1, and iii) SGK1-inh restored cardiac repolarization *ex vivo* in isolated LQT2 and LQT3 hearts. Together, these findings demonstrate that SGK1-inhibition exerts a beneficial cardiac repolarization shortening and antiarrhythmic effect in LQT2 and LQT3 by reducing the enhanced late I_{Na}, and further underscore a role of increased late I_{Na} also in the pathophysiology of the LQT2 phenotype.

Despite advances in clinical management, current LQTS strategies primarily focus on preventing triggers or terminating arrhythmias [30], but ventricular arrhythmias and SCD can still occur in LQTS patients. While life-threatening therapeutic failures may be relatively rare in the common types of LQT1–2–3 for which ICDs are rarely required [31,32], they still represent a serious problem in specific high-risk subgroups insufficiently protected by current standard therapy, including infants with events in the first year of life [33] and patients with malignant variants, particularly in the setting of LQT2 and LQT3.

Pharmacological strategies have attempted to restore physiological QT/APD by employing I_{Ks}-activating compounds such as poly-unsaturated acids or endocannabinoids [28,34–36]. However, this strategy has limited applicability as it cannot be applied in LQTS subtypes associated with deficient *KCNQ1*/I_{Ks} or *KCNE1*/I_{Ks} function (e.g., LQT1 and LQT5) and it provides only partial improvement in genotypes with normal I_{Ks} (such as LQT2) since it does not target the actual defect but only enhances the reduced repolarization reserve [28,35]. In fact, only a few compounds show variant-specific rescue effects depending on the location of the *KCNQ1* variants [34]. Additional strategies have explored targeting late I_{Na}, particularly in LQT3, in which augmented late I_{Na} is a primary defect caused by the pathogenic *SCN5A* variant. Compounds such as ranolazine and mexiletine can reduce late I_{Na} and also have an antiarrhythmic effect [37], but they do not shorten QTc in all LQT3 [37] or LQT2 patients [38], thus leaving room for improvement [39–41]. These limitations of both primary-defect I_{Ks}-activators and late I_{Na} blockers have led to growing interest in therapeutic approaches that target pathways modulating ion channel function. For instance, targeting the disturbances in intracellular Na^+ and Ca^{2+} homeostasis observed in both LQT2 and LQT3 [42,43] may have beneficial effects on both repolarization and arrhythmogenesis. We therefore explored pharmacological inhibition of serum-and glucocorticoid-regulated kinase 1 (SGK1) as a potentially more generalizable approach targeting the secondary intracellular remodelling in the setting of LQTS.

The therapeutic potential of SGK1-inhibition was first demonstrated by Bezzerides et al., who reported that it was able to shorten APD in patient-specific LQT3 hiPSC-CMs [16]. Building on this, we previously showed that SGK1-inhibition shortened APD (by 20–30%) across several LQT2 models, e.g., hiPSC-CMs, cardiac cell sheets (hiPSC-CCS), and transgenic rabbits independent of the underlying *KCNH2* variants [17]. Conversely, the effects of SGK1-inhibition in LQT1 appeared more complex, showing variable responses in the three different *KCNQ1* variants investigated (ranging from no effect on APD in some variants to a shortening of APD in others), suggesting potential variant-specific responses [17]. While another study from Kim et al. [14,15] demonstrated an SGK1-inhibitor dependent cellular APD shortening in

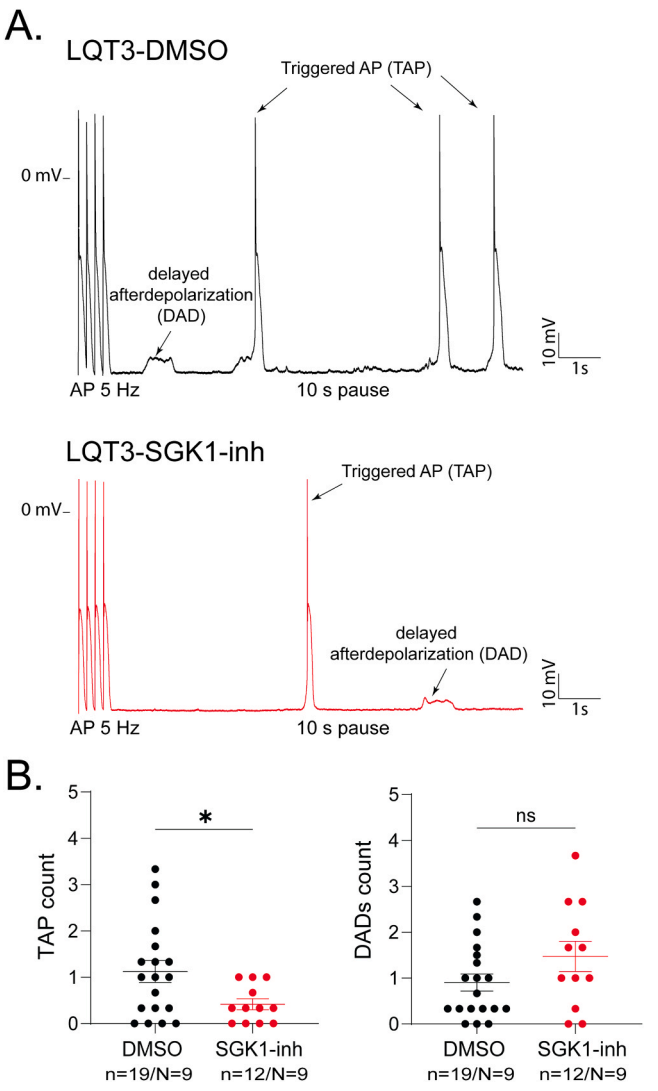

Fig. 4. Effects of SGK1-inh on triggered activity in LQT3 mice CMs. (A) Typical examples of delayed afterdepolarizations (DADs) and triggered APs (TAPs) evoked using a fast pacing stimulation protocol (20 pulses at 5 Hz followed by a 10 s pause) in LQT3 CMs after DMSO or SGK1-inh (300 nM) incubation. The last four elicited APs are shown and DADs and TAPs are indicated by arrows. (**B**) Numbers of DADs and TAPs observed in DMSO or SGK1-inh incubated LQT3 CMs. Average values were calculated using 3 consecutive traces. n, number of CMs, N, number of animals. *$p < 0.05$, nested t-test; ns = non-significant.*

patient-specific hiPSC-CMs models of LQT1, LQT2, and LQT3, it only investigated one pathogenic *KCNQ1* variant [14,15]. Thus, it remains uncertain whether the efficacy is due to the different molecules tested, the specific properties of the *KCNQ1* variant studied and its resulting conformal changes in the KCNQ1 complex which may impact on the channels responsiveness to SGK-Inh [43], the presence (if any) of a variant-related enhanced late I_{Na}, and the degree and nature of associated AP prolongation. Here, we confirm and extend our previous findings by demonstrating that SGK1-inhibition shortens the prolonged cellular APD by approximately 25% in LQT2 CMs and by 23% in LQT3 CMs, resulting in complete normalization of APD relative to WT . Crucially, *ex vivo* studies further demonstrated that SGK1-inhibition normalized QT and ERP in isolated LQT2 and LQT3 hearts, but has no effect in WT, confirming that its effect extends beyond the cellular level.

SGK1 is a known modulator of the cardiac $Na_v1.5$ channel [44], which governs the AP upstroke and contributes to the plateau and repolarization phase of the AP through the late I_{Na} [45,46]. Constitutive SGK1 activation in cardiomyocytes leads to APD prolongation, early and delayed afterdepolarizations (EADs and DADs), and increased late I_{Na}, thus recapitulating features of the LQTS phenotype. These effects were reversible by the late I_{Na}-blocker ranolazine, indicating their dependence on late I_{Na} [13]. SGK1-mediated effects have been attributed to its interaction with $Na_v1.5$ leading to phosphorylation at SGK1 consensus sites and altered channel biophysics [13,16], enhancing Na^+ influx and intracellular Na^+ accumulation, which in turn promotes Ca^{2+} entry via reverse-mode Na^+/Ca^{2+} exchange [47]. A vicious positive feedback loop may develop, wherein increased intracellular Ca^{2+} further augments late I_{Na} via the Ca^{2+}-calmodulin (CaM). Specifically, Ca^{2+}-activated CaM forms a complex that activates the CaM-dependent protein kinase kinase (CaMKK) pathway, which directly phosphorylates SGK1, leading to its enhanced activation and consequently to enhancement in late I_{Na} [48]. Thus, SGK1-inhibition is expected to reduce late I_{Na} and restore repolarization by interrupting this pathological signal cascade. Bezzerides et al., provided the first proof-of-concept of how pharmacological SGK1-inhibition could reduce the native late I_{Na} current in neonatal rat ventricular myocytes, pointing to SGK1-inhibition as a therapeutic target for treating cardiac pathologies associated with augmented late I_{Na} [16]. Consistent with this data, we confirm that SGK1-inhibition significantly reduces late I_{Na} in LQT3 cardiomyocytes (by 33%), resulting in a 23% reduction in APD and complete normalization of cellular repolarization to the WT level. Because LQT3 arises from *SCN5A* gain-of-function variants that directly increase late I_{Na} [19], these data demonstrate that SGK1-dependent modulation of $Na_v1.5$ contributes to the phenotype.

In addition to LQT3, enhanced late I_{Na} is also increasingly implicated in LQT2. Several studies suggest that prolonged APD and altered Ca^{2+} handling in LQT2 result in increased cellular Na^+ and Ca^{2+} loading, which may promote Ca^{2+}-mediated enhancement of late I_{Na} [49,50]. The beneficial effects of late I_{Na} blockers in LQT2 further support this notion: ranolazine shortens APD and prevents EADs in LQT2 hiPSC-CMs [51], the I_{Na} blocker GS-967 suppresses polymorphic VT formation in transgenic LQT2 rabbit hearts by reducing Ca^{2+}-mediated EADs [49], and mexiletine shortens APD and QTc and reduces arrhythmia burden in both experimental LQT2 hiPSC-CMs and rabbit models and LQT2 patients [38]. Together, these findings point toward secondary late I_{Na} enhancement as a contributor to the LQT2 phenotype. Here, we provide direct evidence that late I_{Na} is significantly increased in LQT2 cardiomyocytes. Importantly, SGK1-inhibition reduced this increased late I_{Na} and shortened/normalized APD to WT levels, providing a mechanistic explanation for our earlier observations and identifying SGK1-dependent late I_{Na} enhancement as a shared pathogenic mechanism in LQT2 and LQT3. Whether the observed APD shortening by SGK1-inh is fully explained by the attenuation of late I_{Na} remains unknown, as potential effects of SGK1 on other ionic currents cannot be excluded. Nevertheless, because repolarization reserve is impaired in LQTS, a SGK1-inh induced reduction in the depolarizing late I_{Na} during the plateau phase - when the membrane impedance is high - is expected to have a pronounced effect on APD [52,53]. This mechanism could therefore account for the observed strong SGK1-inh induced APD shortening. In contrast to LQT2 and LQT3, late I_{Na} was not increased in LQT1 rabbit cardiomyocytes compared to WT, which aligns with the lack of APD response to SGK1-inhibition in this model. Late I_{Na} may however be increased in LQT1 cardiomyocytes carrying other *KCNQ1* variants than our LQT1 rabbit model as suggested by the variable APD-shortening efficacy in LQT1 hiPSC-CMs with the same SGK1-inh in our previous study [17] or a different SGK1-inh [14,15].

Under physiological conditions, ventricular repolarization reflects a fine balance between inward and outward currents during the plateau and repolarization phases of the AP. Increased late I_{Na} disrupts this balance, prolongs APD, and promotes intracellular Na^+ and Ca^{2+} accumulation, leading to sarcoplasmic reticulum Ca^{2+} overload, spontaneous release events, and triggered activity [54,55]. These mechanisms contribute to EADs and DADs [42,56], which act as triggers for ventricular arrhythmias, particularly in conditions such as bradycardia or

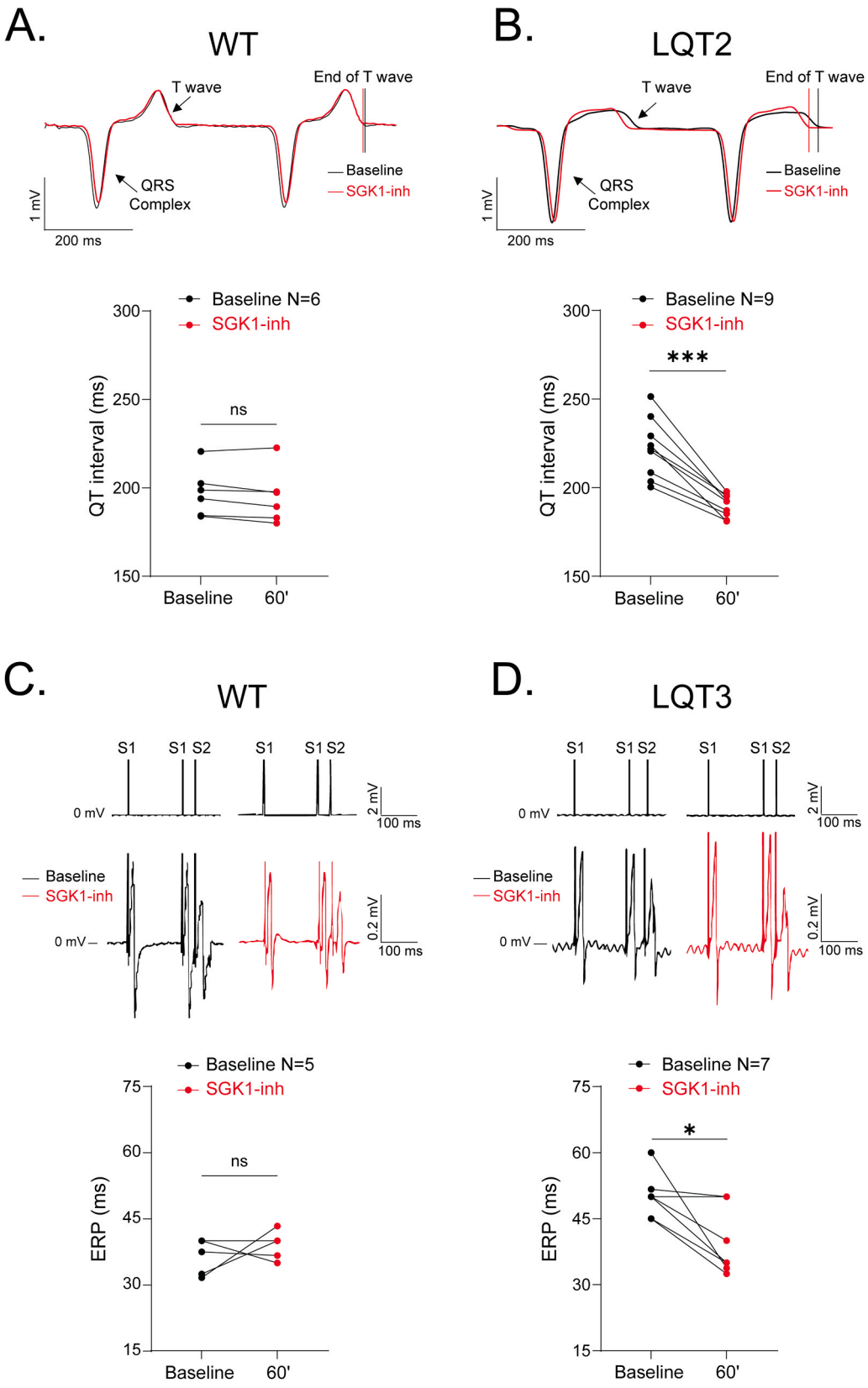

Fig. 5. SGK1-inh shortens the QT interval in LQT2 and the ventricular effective refractory period (ERP) in LQT3 isolated hearts. (A-B) Representative ECG traces of two consecutive beats in ventricular escape rhythm after atrio-ventricular node ablation (upper panels) and corresponding average QT interval at baseline (DMSO) and after 60 min (60') perfusion of SGK1-inh (3 μM; bottom panels) in *ex vivo* Langendorff-perfused hearts from WT (**A**) and LQT2 (**B**) rabbits. (**C-D**) Typical example of ECG recordings (upper panels) in WT (**C**) and LQT3 (**D**) mouse explanted hearts during an ERP protocol at baseline (DMSO, black) and after 60 min (60') perfusion of SGK1-inh (300 nM; red). ERP was determined by reducing the coupling interval of a premature stimulus (after 36 stimuli at basic cycle length of 150 ms) in steps of 5 ms until activation of the ventricle failed. Bottom panels: average ERP in WT (C) and LQT3 (D) explanted mouse hearts. N, number of animals. *$***p < 0.001$*, *$*p < 0.05$*, *paired Student's t-test, ns = non-significant.*

repolarization heterogeneity characteristic of LQTS [57–59]. Consequently, increased late I_{Na} has been recognized as a key proarrhythmic mechanism contributing to the electrical instability observed in both congenital and acquired LQTS. Accordingly, therapeutic strategies that reduce late I_{Na} are expected to have antiarrhythmic effect and to suppress triggered activity [24]. Consistent with this concept, SGK1-inhibition decreased STV of APD, a marker of proarrhythmic risk, in both LQT2 and LQT3 CMs, but not in LQT1. DADs and triggered activity were frequent in LQT3 CMs, and triggered action potentials were significantly reduced by SGK1-inhibition, further supporting its antiarrhythmic potential.

4.1. Limitations and outlook

The precise molecular mechanism by which SGK1-inhibition shortens the APD/QT in LQT2 and LQT3 and, particularly, the reasons for its lack of effect in LQT1, require further investigation. While our data support a direct SGK1-inhibitor effect through late I_{Na} suppression, additional studies are needed to explore other SGK1-dependent pathways and to confirm these effects *in vivo*. Furthermore, long-term studies assessing the safety and chronic efficacy of SGK1-inhibition in humans are warranted. In 2026 a phase 2/3 clinical study evaluating efficacy and safety of an oral SGK1-inhibitor (THRV-1268) in LQT2 patients will commence (https://clinicaltrials.gov/study/NCT07277582).

5. Conclusion

This study demonstrated the ability of pharmacological SGK1-inhibition to shorten and normalize APD/QT, thereby decreasing arrhythmic risk in LQT2 and LQT3 models through reduction of enhanced late I_{Na}. In contrast, no effect was observed in the *KCNQ1*-Y315S LQT1 rabbit model, consistent with the absence of increased late I_{Na}, indicating a subtype-specific efficacy. In line with the cellular data, SGK1-inhibition also improved cardiac repolarization in isolated LQT2 and LQT3 hearts, confirming its beneficial effect at the organ level. Collectively, these findings identify SGK1-inhibition as a promising mechanistic and potentially subtype-selective therapeutic strategy for LQT2 and LQT3 patients, particularly those who remain symptomatic despite standard treatments such as beta-blockers.

CRediT authorship contribution statement

Carol A Remme: Writing – original draft, Supervision, Funding acquisition, Conceptualization. **Luca Sala:** Writing – review & editing. **Katja E Odening:** Writing – original draft, Supervision, Funding acquisition, Conceptualization. **Federica Giannetti:** Writing – review & editing, Data curation. **Arthur AM Wilde:** Writing – review & editing. **Peter J Schwartz:** Writing – review & editing. **Nicolò Alerni:** Writing – review & editing, Data curation. **Lia Crotti:** Writing – review & editing. **Tanja M de Waal:** Formal analysis, Data curation. **Lior Gepstein:** Writing – review & editing. **Julien Louradour:** Writing – review & editing, Validation, Data curation. **Michael Brunner:** Writing – review & editing. **Simona Casini:** Writing – original draft, Visualization, Formal analysis, Conceptualization. **Manfred Zehender:** Writing – original draft. **Miriam Barbieri:** Writing – original draft, Visualization, Formal analysis, Data curation. **Gideon Koren:** Writing – review & editing. **Saumya Das:** Writing – review & editing. **Philip T Sager:** Writing – review & editing. **Arie O Verkerk:** Writing – review & editing, Formal analysis, Data curation.

Funding

This research was funded by the Netherlands CardioVascular Research Initiative (CVON-PREDICT2 2018–30) (to CAR) and a European Joint Research Program on Rare Diseases (EJP-RD) grant 'Silence-LQTS' (to CAR, KEO, LC, AAMW, LG).

Disclosures

SD is a founder and holds equity in Thryv Therapeutics. He is a consultant for Thryv Therapeutics. SD also has equity in Switch Therapeutics and research grants from Cytokinetics, none of which were relevant to this study. PTS is a founder and holds equity in Thryv Therapeutics.

Declaration of Competing Interest

The authors declare that they have no known competing financial interests or personal relationships that could have appeared to influence the work reported in this paper.

Acknowledgements

Miriam Barbieri and Katja Odening thank András Horváth for his valuable electrophysiological contributions. AAMW, LC, and PJS are members of the European Reference Network for rare, low prevalence and complex diseases of the heart: ERN GUARD-Heart (ERN GUARD-HEART; http://guardheart.ern-net.eu).

Appendix A. Supporting information

Supplementary data associated with this article can be found in the online version at doi:10.1016/j.phrs.2026.108189.

Data availability

The data that support the findings of this study are available from the corresponding authors upon reasonable request

References

[1] P.J. Schwartz, L. Crotti, Long QT syndrome, N. Engl. J. Med 393 (2025) 2023–2033.
[2] S. Nimani, M. Barbieri, M. 3 Rieder, K.E. Odening, Current and future precision therapy approaches in the long QT syndrome, Med Genet 37 (2025) 189–196.
[3] M. Ackerman, D.L. Atkins, J.K. Triedman, Sudden Cardiac Death in the Young, Circulation 133 (2016) 1006–1026.
[4] M.J. Ackerman, S.G. Priori, S. Willems, C. Berul, R. Brugada, H. Calkins, A. J. Camm, P.T. Ellinor, M. Gollob, R. Hamilton, R.E. Hershberger, D.P. Judge, H. Le Maree, W.J. McKenna, E. Schulze-Bahr, C. Semsarian, J.A. Towbin, H. Watkins, A. A.M. Wilde, C. Wolpert, D.P. Zipes, HRS/EHRA expert consensus statement on the state of genetic testing for the channelopathies and cardiomyopathies, Heart Rhythm 8 (2011) 1308–1339.
[5] J.D. Kapplinger, D.J. Tester, B.A. Salisbury, J.L. Carr, C. Harris-Kerr, G. D. Pollevick, A.A.M. Wilde, M.J. Ackerman, Spectrum and prevalence of mutations from the first 2,500 consecutive unrelated patients referred for the FAMILION® long QT syndrome genetic test, Heart Rhythm 6 (2009) 1297–1303.
[6] L. Crotti, P. Brugada, H. Calkins, P. Chevalier, G. Conte, G. Finocchiaro, P. G. Postema, V. Probst, P.J. Schwartz, E.R. Behr, From gene-discovery to gene-tailored clinical management: 25 years of research in channelopathies and cardiomyopathies, Europace 25 (2023) euad180.
[7] C.A. Remme, A.A. Wilde, Late sodium current inhibition in acquired and inherited ventricular (dys)function and arrhythmias, Cardiovasc Drugs Ther. 27 (2013) 91–100.
[8] J.F. Liu, C. Jons, A.J. Moss, S. McNitt, D.R. Peterson, M. Qi, W. Zareba, J. L. Robinson, A. Barsheshet, M.J. Ackerman, J. Benhorin, E.S. Kaufman, E.H. Locati, C. Napolitano, S.G. Priori, P.J. Schwartz, J. Towbin, M. Vincent, L. Zhang, I. Goldenberg, Risk factors for recurrent syncope and subsequent fatal or near-fatal events in children and adolescents with long QT syndrome, J. Am. Coll. Cardiol. 57 (2011) 941–950.
[9] P.J. Schwartz, R.L. Woosley, Predicting the unpredictable: drug-induced QT prolongation and torsades de pointes, J. Am. Coll. Cardiol. 67 (2016) 1639–1650.
[10] G. Mennig, J. Kobe, A. Laher, L. Eckardt, H. Wedekind, H.H. Scheid, W. Haverkamp, P. Milberg, G. Breithardt, E. Schulze-Bahr, D. Bocker, Implantable cardioverter-defibrillator therapy in patients with congenital long-QT syndrome: a long-term follow-up, Heart Rhythm 2 (2005) 497–504.
[11] P.J. Schwartz, C. Spazzolini, S.G. Priori, L. Crotti, A. Vicentini, M. Landolina, M. Gasparini, A.A.M. Wilde, R.E. Knops, I. Denjoy, L. Toivonen, G. Mennig, M. Al-Fayyadh, L. Jordaens, M. Borggrefe, C. Holmgren, P. Brugada, L. De Roy, S. H. Hohnloser, P.A. Brink, Who are the long-QT syndrome patients who receive an implantable cardioverter-defibrillator and what happens to them? Circulation 122 (2010) 1272–1282.

[12] V. Dusi, L. Pugliese, G.M. De Ferrari, A. Odero, L. Crotti, F. Dagradi, S. Castelletti, A. Vicentini, R. Rordorf, C. Li, M. Shkolnikova, C. Spazzolini, P.J. Schwartz, Left cardiac sympathetic denervation for Long QT syndrome: 50 years' experience provides guidance for management. JACC Clin Electrophysiol 8 (2022) 281–294.
[13] S. Das, T. Aiba, M. Rosenberg, K. Hessler, C. Xiao, P.A. Quintero, F.G. Ottaviano, A. C. Knight, E.L. Graham, P. Bostrom, M.R. Morissette, F. del Monte, M.J. Begley, L. C. Cantley, P.T. Ellinor, G.F. Tomaselli, A. Rosenzweig, Pathological role of serum- and glucocorticoid-regulated kinase 1 in adverse ventricular remodeling, Circulation 126 (2012) 2208–2219.
[14] M. Kim, P.T. Sager, D.J. Tester, S. Pradhananga, S.K. Hamrick, D. Srinivasan, S. Das, M.J. Ackerman, SGK1 inhibition attenuates the action potential duration in reengineered heart cell models of drug-induced QT prolongation, Heart Rhythm 20 (2023) 589–595.
[15] M. Kim, S. Das, D.J. Tester, S. Pradhananga, S.K. Hamrick, X. Gao, D. Srinivasan, P. T. Sager, M.J. Ackerman, SGK1 inhibition attenuated the action potential duration in patient- and genotype-specific re-engineered heart cells with congenital long QT syndrome, Heart Rhythm (2023).
[16] V.J. Bezzerides, A. Zhang, L. Xiao, B. Simonson, S.A. Khedkar, S. Baba, F. Ottaviano, S. Lynch, K. Hessler, A.C. Rigby, D. Milan, S. Das, A. Rosenzweig, Inhibition of serum and glucocorticoid regulated kinase-1 as novel therapy for cardiac arrhythmia disorders, Sci. Rep. 7 (2017) 346.
[17] F. Giannetti, M. Barbieri, A. Shiti, S. Casini, P.T. Sager, S. Das, S. Pradhananga, D. Srinivasan, S. Nimani, N. Alerni, J. Louradour, M. Mura, M. Gnecchi, P. Brink, M. Zehender, G. Koren, A. Zaza, L. Crotti, M.M. Wilde, P.J. Schwartz, C.A. Remme, L. Gepstein, L. Sala, K.E. Odening, Gene- and variant-specific efficacy of serum/glucocorticoid-regulated kinase 1 inhibition in Long QT syndrome types 1 and 2, Europace 25 (2023) euad094.
[18] M. Brunner, X. Peng, G.X. Liu, X.O. Ren, O. Ziv, B.R. Choi, R. Mathur, M. Hajjiri, K. E. Odening, E. Steinberg, E.J. Folco, E. Pringa, J. Centracchio, R.R. Macharzina, T. Donahay, L. Schofield, N. Rana, M. Kirk, G.F. Mitchell, A. Poppas, M. Zehender, G. Koren, Mechanisms of cardiac arrhythmias and sudden death in transgenic rabbits with Long QT syndrome, J. Clin. Invest 118 (2008) 2246–2259.
[19] C.A. Remme, A.O. Verkerk, D. Nuyens, A.G.C. van Ginneken, S. van Brunschot, C. N.W. Belterman, M.A. van Roon, H.L. Tan, M.M. Wilde, P. Carmeliet, J.M.T. de Bakker, M.W. Veldkamp, C.R. Bezzina, Overlap syndrome of cardiac sodium channel disease in mice carrying the equivalent mutation of human SCN5A-1795insD, Circulation 114 (2006) 2584–2592.
[20] C.A. Remme, B.P. Scicluna, A.O. Verkerk, A.S. Amin, S. van Brunschot, L. Beekman, V.H.M. Deneer, C. Chevalier, F. Oyama, H. Miyazaki, N. Nukina, R. Wilders, D. Escande, R. Houlgatte, M.M. Wilde, H.L. Tan, M.W. Veldkamp, J.M.T. de Bakker, C.R. Bezzina, Genetically determined differences in sodium current characteristics modulate conduction disease severity in mice with cardiac sodium channelopathy, Circ. Res 104 (2009) 1283–1292.
[21] K.E. Odening, O. Hyder, L. Chaves, L. Schofield, M. Brunner, M. Kirk, M. Zehender, X. Peng, G. Koren, Pharmacogenomics of anesthetic drugs in transgenic LQT1 and LQT2 rabbits reveal genotype-specific differential effects on cardiac repolarization, Am. J. Physiol. Heart Circ. Physiol. 295 (2008) H2264–H2272.
[22] S. Bains, L. Giammarino, S. Nimani, N. Alerni, D.J. Tester, C.S.J. Kim, N. Christoforou, J. Louradour, A. Horvath, O. Beslac, M. Barbieri, L. Matas, T. S. Hof, R. Lopez, S. Perez-Feliz, C. Parodi, L.G. Garcia Casalta, J. Jurgensen, M. A. Barry, M. Sego, L. Keyes, J. Owens, J. Pinkstaff, G. Koren, M. Zehender, M. Brunner, D. Casoni, F. Praz, A. Haeberlin, G. Brooks, M.J. Ackerman, K. E. Odening, KCNQ1 suppression-replacement gene therapy in transgenic rabbits with type 1 Long QT syndrome, Eur. Heart J. 45 (2024) 3751–3763.
[23] P.H. Barry, J.W. Lynch, Liquid junction potentials and small cell effects in patch-clamp analysis, J. Membr. Biol. 121 (1991) 101–117.
[24] V. Portero, S. Casini, M. Hoekstra, A.O. Verkerk, I. Mengarelli, L. Belardinelli, S. Rajamani, A.A.M. Wilde, C.R. Bezzina, M.W. Veldkamp, C.A. Remme, Anti-arrhythmic potential of the late sodium current inhibitor GS-458967 in murine Scn5a-1798insD+/− and human SCN5A1795insD+/− iPSC-derived cardiomyocytes, Cardiovasc Res 113 (2017) 829–838.
[25] B. Hegyi, S. Marotti, C. Liu, K.S. Ginsburg, J. Bossuyt, L. Belardinelli, L.T. Izu, Y. Chen-Izu, T. Banyasz, E. Grandi, D.M. Bers, Enhanced depolarization drive in failing rabbit ventricular myocytes, Circ. Arrhythm. Electro 12 (2019) e007061.
[26] D. Ziupa, J. Beck, G. Franke, S. Perez Feliz, M. Hartmann, G. Koren, M. Zehender, C. Bode, M. Brunner, K.E. Odening, Pronounced effects of HERG-blockers E-4031 and erythromycin on APD, spatial APD dispersion and triangulation in transgenic Long-QT type 1 rabbits, PLoS One 9 (2014) e107210.
[27] K.E. Odening, B.A. Jung, C.N. Lang, R.C. Lozoya, D. Ziupa, M. Menza, J. Relan, G. Franke, S. Perez Feliz, G. Koren, M. Zehender, C. Bode, M. Brunner, M. Sermesant, D. Foll, Spatial correlation of action potential duration and diastolic dysfunction in transgenic and drug-induced LQT2 rabbits, Heart Rhythm 10 (2013) 1533–1541.
[28] J. Louradour, T. Hornyik, A. De la Cruz, I. Hiniesto-Iriigo, N. Alerni, M. Barbieri, R. Lopez, S. Perez-Feliz, L. Matas, S. Nimani, L. Giammarino, G. Koren, M. Zehender, M. Brunner, S.I. Liin, H.P. Larsson, K.E. Odening, Beneficial action potential duration-shortening effects, but deleterious negative inotropism of IKs-activator docosahexaenoyl glycine in long QT syndrome type 2, Europace 27 (2025) euaf168.
[29] R. Varkevisser, S.C. Wijers, M.A.G. van der Heyden, J.D.M. Beekman, M. Meine, M. A. Vos, Beat-to-beat variability of repolarization as a new biomarker for proarrhythmia in vivo, Heart Rhythm 9 (2012) 1718–1726.
[30] P.J. Schwartz, S.G. Priori, M. Cerrone, C. Spazzolini, A. Odero, C. Napolitano, R. Bloise, G.M. De Ferrari, C. Klersy, A.J. Moss, W. Zareba, J.L. Robinson, W. J. Hall, P.A. Brink, L. Toivonen, A.E. Epstein, C. Li, D. Hu, Left cardiac sympathetic denervation in the management of high-risk patients affected by the long-QT syndrome, Circulation 109 (2004) 1826–1833.
[31] V. Dusi, F. Dagradi, C. Spazzolini, L. Crotti, P. Cerea, F.L.F. Giovenzana, G. Musu, M. Pedrazzini, M. Torchio, P.J. Schwartz, Long QT syndrome: importance of reassessing arrhythmic risk after treatment initiation, Eur. Heart J. 45 (2024) 2647–2656.
[32] R. Neves, L. Crotti, S. Bains, J.M. Bos, D. Ye, F. Dagradi, G. Musu, F. Spiezia, M. Pedrazzini, F.L.F. Giovenzana, P. Cerea, J.R. Giudicessi, P.J. Schwartz, M. J. Ackerman, A phenotype-enhanced variant classification framework to decrease the burden of variants of uncertain significance in type 2 long QT syndrome, JACC Clin. Electro (2025). S2405-500X(25)00825-4.
[33] C. Spazzolini, J. Mullally, A.J. Moss, P.J. Schwartz, S. McNitt, G. Ouellet, T. Fugate, I. Goldenberg, C. Jons, W. Zareba, J.L. Robinson, M.J. Ackerman, J. Benhorin, L. Crotti, E.S. Kaufman, E.H. Locati, M. Qi, C. Napolitano, S.G. Priori, J.A. Towbin, G.M. Vincent, Clinical implications for patients with long QT syndrome who experience a cardiac event during infancy, J. Am. Coll. Cardiol. 54 (2009) 832–837.
[34] I. Hiniesto-Iriigo, A. Sridhar, J. Louradour, A. De la Cruz, S. Lundholm, A. Jauregi-Miguel, F. Giannetti, L. Sala, K.E. Odening, H.P. Larsson, N.E. Ottosson, S.I. Liin, Rescue of loss-of-function long QT syndrome-associated mutations in Kv7.1/KCNE1 by the endocannabinoid N-arachidonoyl-L-serine (ARA-S), Br. J. Pharm. 182 (2025) 2861–2877.
[35] A. Castiglione, T. Hornyik, E.M. Wulfers, L. Giammarino, I. Edler, J.J. Jowais, M. Rieder, S. Perez-Feliz, G. Koren, Z. Bősze, A. Varró, M. Zehender, M. Brunner, C. Bode, S.I. Liin, H.P. Larsson, I. Baczkó, K.E. Odening, Docosahexaenoic acid normalizes QT interval in long QT type 2 transgenic rabbit models in a genotype-specific fashion, Europace 24 (2022) 511–522.
[36] M.A. Skarsfeldt, S.I. Liin, H.P. Larsson, B.H. Bentzen, Polyunsaturated fatty acid-derived IKs channel activators shorten the QT interval ex-vivo and in-vivo, Acta Physiol. 229 (2020) e13471.
[37] A. Mazzanti, R. Maragna, A. Faragli, N. Monteforte, R. Bloise, M. Memmi, V. Novelli, P. Baiardi, V. Bagnardi, S.P. Etheridge, C. Napolitano, S.G. Priori, Gene-specific therapy with mexiletine reduces arrhythmic events in patients with Long QT syndrome type 3, J. Am. Coll. Cardiol. 67 (2016) 1053–1058.
[38] L. Crotti, R. Neves, F. Dagradi, G. Musu, F. Giannetti, J.M. Bos, M. Barbieri, P. Cerea, F.L.F. Giovenzana, M. Torchio, M. Mura, M. Gnecchi, G. Conte, A. Auricchio, L. Sala, K.E. Odening, M.J. Ackerman, P.J. Schwartz, Therapeutic efficacy of mexiletine for Long QT syndrome type 2, Circulation 150 (2024) 531–543.
[39] G. Li, R.L. Woltz, C. Wang, L. Ren, P. He, S. Yu, X. Liu, V. Yarov-Yarovoy, D. Hu, N. Chiamvimonvat, L. Wu, Gating properties of mutant sodium channels and responses to sodium current inhibitors predict mexiletine-sensitive mutations of Long QT syndrome 3, Front Pharm. 11 (2020) 1182.
[40] J.D. Moreno, C.E. Clancy, Pathophysiology of the cardiac late Na current and its potential as a drug target, J. Mol. Cell Cardiol. 52 (2011).
[41] C.A. Remme, A.A.M. Wilde, Targeting sodium channels in cardiac arrhythmia, Curr. Opin. Pharm. 15 (2014) 53–60.
[42] M.R. Rivaud, A. Baartscheer, A.O. Verkerk, L. Beekman, S. Rajamani, L. Belardinelli, C.R. Bezzina, C.A. Remme, Enhanced late sodium current underlies pro-arrhythmic intracellular sodium and calcium dysregulation in murine sodium channelopathy, Int J. Cardiol. 263 (2018) 54–62.
[43] D. Terentyev, C.M. Rees, W. Li, L.L. Cooper, H.K. Jindal, X. Peng, Y. Lu, R. Terentyeva, K.E. Odening, J. Daley, K. Bist, B.R. Choi, A. Karma, G. Koren, Hyperphosphorylation of RyRs underlies triggered activity in transgenic rabbit model of LQT2 syndrome, Circ. Res 115 (2014) 919–928.
[44] G. Seebohm, N. Strutz-Seebohm, O.N. Ureche, U. Henrion, R. Baltaev, A.F. Mack, G. Korniychuk, K. Steinke, D. Tapken, A. Pfeufer, S. Kaab, C. Bucci, B. Attali, J. Merot, J.M. Tavare, U.C. Hoppe, M.C. Sanguinetti, F. Lang, Q.T. Long, syndrome-associated mutations in KCNQ1 and KCNE1 subunits disrupt normal endosomal recycling of IKs channels, Circ. Res 103 (2008) 1451–1457.
[45] C. Boehmer, V. Wilhelm, M. Palmada, S. Wallisch, G. Henke, H. Brinkmeier, P. Cohen, B. Pieske, F. Lang, Serum and glucocorticoid inducible kinases in the regulation of the cardiac sodium channel SCN5A, Cardiovasc Res 57 (2003) 1079–1084.
[46] S. Niederer, Regulation of ion gradients across myocardial ischemic border zones: a biophysical modelling analysis, PLoS One 8 (2013) e60323.
[47] V.A. Maltsev, H.N. Sabbah, R.S. Higgins, Novel ultraslow inactivating sodium current in human ventricular cardiomyocytes, Circulation 98 (1998) 2545–2552.
[48] K. Kistamas, T. Hezso, B. Horvath, P.P. Nanasi, Late sodium current and calcium homeostasis in arrhythmogenesis, Channels 15 (2020) 1–19.
[49] S. Imai, N. Okayama, M. Shimizu, M. Itoh, Increased intracellular calcium activates serum- and glucocorticoid-inducible kinase 1 through a CaMKK pathway in CHO cells, Life Sci. 72 (2003) 2199–2209.
[50] J. Hwang, T.Y. Kim, D. Terentyev, M. Zhong, A.Y. Kabakov, P. Bronk, K. Arunachalam, L. Belardinelli, S. Rajamani, Y. Kunitomo, Z. Pfeiffer, Y. Lu, X. Peng, K.E. Odening, Z. Ou, A. Karma, G. Koren, B.R. Choi, Late INa blocker GS967 suppresses polymorphic ventricular tachycardia in a transgenic rabbit model of LQT2, Circ. Arrhythm. Electro 13 (2020) e006875.
[51] I. Itzhaki, L. Maizels, I. Huber, L. Zwi-Dantsis, O. Caspi, A. Winterstern, O. Feldman, A. Gepstein, G. Arbel, H. Hammerman, M. Boulos, L. Gepstein, Modelling the Long QT syndrome with induced pluripotent stem cells, Nature 471 (2011) 225–229.
[52] B. Horvath, T. Hezso, D. Kiss, K. Kistamas, J. Magyar, P.P. Nanasi, T. Banyasz, Late sodium current inhibitors as potential antiarrhythmic agents, Front Pharm. 11 (2020) 413.

[53] L. Wu, S. Rajamani, H. Li, C.T. January, J.C. Shryock, L. Belardinelli, Reduction of repolarization reserve unmasks the proarrhythmic role of endogenous late Na current in the heart, Am. J. Physiol. Heart Circ. Physiol. 297 (2009) H1048–H1057.
[54] B. Horvath, T. Banyasz, Z. Jian, B. Hegyi, K. Kistamas, P.P. Nanasi, L.T. Izu, Y. Chen-Izu, Dynamics of the late Na current during cardiac action potential and its contribution to afterdepolarizations, J. Mol. Cell Cardiol. 64 (2013) 59–68.
[55] C.R. Studenik, Z. Zhou, C.T. January, Differences in action potential and early afterdepolarization properties in LQT2 and LQT3 models of Long QT syndrome, Br. J. Pharm. 132 (2001) 85–92.
[56] J.S. Lowe, D.M. Stroud, T. Yang, L. Hall, T.C. Atack, D.M. Roden, Increased late sodium current contributes to Long QT-related arrhythmia susceptibility in female mice, Cardiovasc Res 95 (2012) 300–307.
[57] N. El-Sherif, G. Turitto, M. Boutjdir, Acquired Long QT syndrome and electrophysiology of torsade de pointes, Arrhythm. Electro Rev. 8 (2019) 122–130.
[58] N. Szentandrassy, K. Kistamas, B. Hegyi, B. Horvath, F. Ruzsnavszky, K. Vaczi, J. Magyar, T. Banyasz, A. Varro, P.P. Nanasi, Contribution of ion currents to beat-to-beat variability of action potential duration in canine ventricular myocytes, Pflug. Arch. 467 (2015) 1431–1443.
[59] V.A. Maltsev, N. Silverman, H.N. Sabbah, A.I. Undrovinas, Chronic heart failure slows late sodium current in human and canine ventricular myocytes: implications for repolarization variability, Eur. J. Heart Fail 9 (2007) 219–227.